Damped eigenmode saturation in plasma fluid turbulence

K. D. Makwana, P. W. Terry, J.-H. Kim, and D. R. Hatch

Citation: Phys. Plasmas **18**, 012302 (2011); doi: 10.1063/1.3530186
View online: http://dx.doi.org/10.1063/1.3530186
View Table of Contents: http://pop.aip.org/resource/1/PHPAEN/v18/i1
Published by the American Institute of Physics.

Damped eigenmode saturation in plasma fluid turbulence

K. D. Makwana, P. W. Terry, J.-H. Kim, and D. R. Hatch
Department of Physics, University of Wisconsin-Madison, Madison, Wisconsin 53706, USA

(Received 21 October 2010; accepted 2 December 2010; published online 10 January 2011)

A broad sample of fluid models for instability-driven plasma turbulence is surveyed to determine whether saturation involving damped eigenmodes requires special physics or is a common property of plasma turbulence driven by instability. Previous investigations have focused exclusively on turbulence in the core of tokamak discharges. The models surveyed here apply to a wide range of physical mechanisms for instability, turbulent mode coupling, and parameter regimes, with the common modeling feature that the physics has been reduced to a two-field fluid description. All the models have regimes in which damped eigenmodes saturate the instability by damping the fluctuation energy at a rate comparable to the injection rate by the unstable eigenmode. A test function derived from model parameters is found to predict when damped eigenmodes provide saturation. This confirms that a critical condition for saturation by damped eigenmodes is that the damping rate of the damped eigenmode does not greatly exceed the growth rate. For the quadratic dispersion relation of two-field models, this tends to hold in regimes of stronger instability and for regimes with strong gradients and strong diamagnetic frequency. Nonlinear coupling also matters. Strong coupling can overcome the effects of heavy damping, while weak coupling can prevent a damped eigenmode from saturating turbulence even though it is not heavily damped. This study indicates that damped eigenmodes represent a pervasive mechanism for the saturation of plasma instability in fluid descriptions, complementing recent works showing these effects in comprehensive gyrokinetic models. © *2011 American Institute of Physics*. [doi:10.1063/1.3530186]

I. INTRODUCTION

Plasma instabilities correspond to the root of a linearized dielectric function or dispersion relation. When instability fluctuation amplitudes have grown to finite levels, mode coupling can transfer energy to other roots of the dielectric. If these are damped, energy is removed from the fluctuation spectrum. Dissipation by damped eigenmodes, particularly in the same wave number range as the instability, has been shown to be a significant factor in saturation in a few systems, notably trapped electron mode (TEM) turbulence,[1] ion temperature gradient (ITG) turbulence,[2–4] and electron temperature gradient (ETG) turbulence.[5]

This type of saturation is different from the notion of a wave number cascade, which is generally invoked for saturation because it provides a means for carrying energy from the scales of instability to a distinct set of scales where energy is damped.[6] Even though it is accepted that plasma turbulence need not have inertial scales, i.e., scales where both energy injection and energy dissipation are zero, it is nonetheless thought that energy injection and dissipation reside in separate, albeit perhaps adjacent, scale ranges. However, when damped eigenmodes are excited, mode coupling in wave number space operates to transfer energy from the instability, but it does not have to leave the wave number range of the instability. Damped eigenmodes generally coexist in the same wave number range as the instability and provide a sink for the instability energy. This makes *all* of wave number space a lossy medium and places instability-driven plasma turbulence under a different set of governing principles than the scale invariance considerations of the inertial range in Navier–Stokes turbulence.[7]

The turbulence systems where damped eigenmodes have been shown to play an important role in saturation are limited to core turbulence in tokamaks.[1–5] It is reasonable to inquire as to whether this phenomenon is widespread in plasmas or peculiar to some restricted set of physical processes, parameter regimes, and models. To provide a partial answer to this question, we survey here nine two-field fluid models for plasma turbulence,[8–16] representing a wide range of physical mechanisms for instability, turbulent mode coupling, and parameter regimes. The models describe trapped electron mode turbulence,[8] local Hasegawa–Wakatani turbulence,[9] two-dimensional turbulence driven by the Rayleigh–Taylor instability,[10] local electrostatic resistive g-mode turbulence,[11] ion temperature gradient turbulence,[12] microtearing mode turbulence,[13] a variant of microtearing turbulence with temperature fluctuations,[14] a thermally driven edge drift wave,[15] and an edge drift wave driven by ionization and charge exchange processes.[16] Local models treat the parallel wave number as a constant. These models represent significant variations of physics and key parameters. For example, they sample both electrostatic and electromagnetic fluctuations and involve a variety of other fluctuating fields. They span regimes in temperature from hot to cold, in trapping physics from trapped to untrapped, in field-line configurations from closed to open, and in discharge locale from core to scrape-off layer. While all the models have two fields, there is considerable parametric complexity over the full model set.

A simple quantity has been defined for assessing the likelihood that damped eigenmodes play a significant role in saturation in any given system.[2] Formulated directly from

model parameters, this quantity is an estimate of the relative sizes, in saturation, of the energy transfer rate from unstable to stable eigenmode versus the transfer rate to different wavelengths of the unstable eigenmode only. The latter encompasses the conventional wave number cascade. We calculate the parameter P_t that quantifies this ratio both analytically and numerically. This exercise establishes whether P_t is a good indicator that damped eigenmodes are excited at a level sufficient to impact the energy transfer dynamics and determines the critical value of P_t for this to be the case. We also measure energy dissipation rates to determine whether the damped eigenmode provides a dissipative balance for energy input from the instability and how this correlates with the value of P_t. By varying model parameters and comparing across the nine models of this study, we appraise which aspects of model behavior most influence the value of P_t.

Calculation of P_t and eigenmode energies in saturation shows that when P_t is of the order of a few tenths or larger, the damped eigenmode energies are comparable to the energy of the growing mode. Thus the parameter P_t is a reasonable qualitative indicator of when damped eigenmodes achieve a significant fluctuation level. When P_t is of this magnitude, the dissipation rate by the damped eigenmode is comparable to the energy input rate. The amount of energy dissipated by the growing eigenmode at high k, where its growth rate turns negative, is small. A significant fraction of the energy input is dissipated by the damped eigenmode in the wave number range of the instability and is associated with a finite-amplitude-induced change in the cross phase that governs instability. This implies that damped eigenmodes generally yield sizable reductions of the quasilinear fluxes in reduced models. A smaller fraction of the energy input rate is dissipated by collisional terms, split in similar measures between the collisional dissipation of the unstable and stable eigenmodes.

Analysis of P_t, energies, and energy evolution rates shows that all models have regimes where damped eigenmodes play a significant role in saturating the instability. The input to P_t that has the strongest influence on its value is the ratio of the stable mode damping rate to the unstable mode growth rate. Damped eigenmodes tend to be prominent in saturation when this ratio is between zero and of order unity. In certain cases where the nonlinear transfer to the damped eigenmode is enhanced relative to transfer on the unstable manifold, the damped eigenmode damping balances the energy input even when this ratio varies by as much as 100.

The remainder of this paper is organized as follows. In Sec. II we describe the nine models in a general form and review the parameter P_t and its inputs. In Sec. III we characterize saturation in each model in terms of an analysis of P_t, saturation energies, and energy evolution rates. Section IV examines energetics and transport. Conclusions are given in Sec. V.

II. MODELS AND PRELIMINARY CONSIDERATIONS

The two-field turbulence models we examine[8–16] have the following form:

$$\frac{\partial F_1}{\partial t} + Z_{11}F_1 + Z_{12}F_2 = N_1, \tag{1}$$

$$\frac{\partial F_2}{\partial t} + Z_{21}F_1 + Z_{22}F_2 = N_2, \tag{2}$$

where F_1 and F_2 are the Fourier amplitudes of two fluctuating quantities, Z_{ij} are linear coupling coefficients, and N_1 and N_2 are nonlinearities. Distinct linear behaviors and instabilities are possible through the four linear, complex-valued coupling coefficients Z_{ij}. Even though the dispersion relation is quadratic, its roots are complicated functionals of an eight-dimensional function space. With the exception of the thermal microtearing model with time-dependent thermal force (TDTF),[14] the nonlinearities have the form

$$N_1 = \sum_{k'} [A_1(k,k')F_2(k')F_1(k-k') + B_1(k,k')F_2(k')F_2(k-k')], \tag{3}$$

$$N_2 = \sum_{k'} [A_2(k,k')F_2(k')F_2(k-k') + B_2(k,k')F_2(k')F_1(k-k')], \tag{4}$$

where $A_j(k,k')$ and $B_j(k,k')$ are nonlinear, three-wave coupling coefficients between wave numbers k, k', and $k-k'$. When F_2 is identified with the scalar stream function of an electric or magnetic field (i.e., potential ϕ or flux function ψ), electrostatic models have A-type nonlinearities, with $B_1=B_2=0$ and electromagnetic models have B-type nonlinearities with $A_1=A_2=0$. The second fluctuation F_1 is a scalar such as pressure, density, temperature, or parallel flow. The thermal microtearing model[14] has additional nonlinear couplings represented by $G_1(k,k')F_1(k')F_1(k-k')$ in the equation for N_1 and $G_2(k,k')F_1(k')F_2(k-k')$ in the equation for N_2.

To differentiate energy transfer paths in the hyper space of the eigenmodes, the dynamical equations, Eqs. (1) and (2), must be transformed to the eigenmode decomposition. In the eigenmode decomposition, the dynamical equations are diagonal in the linear coupling and given by

$$\frac{\partial \beta_1(k)}{\partial t} + i\omega_1(k)\beta_1(k) = \sum_{k'} [C_1(k,k')\beta_1(k')\beta_1(k'') + C_2(k,k')\beta_1(k')\beta_2(k'') + C_3(k,k')\beta_1(k'')\beta_2(k') + C_4(k,k')\beta_2(k')\beta_2(k'')], \tag{5}$$

$$\frac{\partial \beta_2(k)}{\partial t} + i\omega_2(k)\beta_2(k) = \sum_{k'} [D_1(k,k')\beta_1(k')\beta_1(k'') + D_2(k,k')\beta_1(k')\beta_2(k'') + D_3(k,k')\beta_1(k'')\beta_2(k') + D_4(k,k')\beta_2(k')\beta_2(k'')], \tag{6}$$

where β_j are the amplitudes of the two linear eigenmodes, $\omega_j(k)$ are the linear eigenfrequencies, and C_j and D_j are linear combinations of the coupling coefficients A_j and B_j weighted by components of the linear eigenvectors. The wave number k'' is $k-k'$. If β_1 is the unstable eigenmode, Im $\omega_1(k)=\gamma_1(k)$ is positive for some range of wave numbers k. If β_2 is a damped eigenmode, Im $\omega_2(k)=\gamma_2(k)$ is negative for all k.

The frequencies $\omega_1(k)$ and $\omega_2(k)$ are roots of the characteristic equation $\omega^2+i(Z_{11}+Z_{22})-Z_{11}Z_{22}+Z_{12}Z_{21}=0$. The growth rates γ_1 and γ_2 are the imaginary parts of the two eigenfrequencies, given by

$$\gamma_{1,2}=-\frac{\mathrm{Re}(Z_{11}+Z_{22})}{2}\pm\frac{1}{2}\mathrm{Re}[(Z_{11}-Z_{22})^2+4Z_{12}Z_{21}]^{1/2}$$
$$=-\frac{b_r}{2}\pm\frac{\rho^{1/2}}{2}\cos\left[\frac{\phi}{2}\right], \tag{7}$$

where

$$b_r=\mathrm{Re}(Z_{11}+Z_{22}),\quad \rho=|4Z_{12}Z_{21}+(Z_{11}-Z_{22})^2|, \tag{8}$$

$$\phi=\tan^{-1}\left\{\frac{\mathrm{Im}[4Z_{12}Z_{21}+(Z_{11}-Z_{22})^2]}{\mathrm{Re}[4Z_{12}Z_{21}+(Z_{11}-Z_{22})^2]}\right\}. \tag{9}$$

The coupling coefficients C_1, C_2, and D_1 mix the original coefficients $A_j(k,k')$ and $B_j(k,k')$ with weights given by the eigenvector components R_1 and R_2

$$R_j(k)=\frac{i\omega_j(k)-Z_{22}}{Z_{21}}, \tag{10}$$

where $\omega_j=\omega_{jr}+i\gamma_j$, with γ_j given by Eq. (7) and ω_{jr} given by

$$\omega_{1,2r}=\frac{\mathrm{Im}(Z_{11}+Z_{22})}{2}\pm\frac{\rho^{1/2}}{2}\sin\left[\frac{\phi}{2}\right]. \tag{11}$$

In terms of these quantities we have

$$C_1(k,k')=C_3(k,k')$$
$$=\frac{Z_{21}}{[(Z_{11}-Z_{22})^2+4Z_{12}Z_{21}]^{1/2}}[A_1(k,k')R_1(k'')$$
$$+B_1(k,k')-R_2(k)[A_2(k,k')$$
$$+R_1(k'')B_2(k,k')]], \tag{12}$$

where it is understood that Z_{ij} are functions of k unless they appear in $R_j(k'')$, in which case they and ω_j are functions of k''. The remaining coefficients are

$$C_2(k,k')=\frac{Z_{21}}{[(Z_{11}-Z_{22})^2+4Z_{12}Z_{21}]^{1/2}}\{A_1(k,k')R_2(k'')$$
$$+B_1(k,k')-R_2(k)[A_2(k,k')$$
$$+R_2(k'')B_2(k,k')]\}, \tag{13}$$

$$D_1(k,k')=\frac{Z_{21}}{[(Z_{11}-Z_{22})^2+4Z_{12}Z_{21}]^{1/2}}\{A_1(k,k')R_1(k'')$$
$$+B_1(k,k')-R_1(k)[A_2(k,k')$$
$$+R_1(k'')B_2(k,k')]\}. \tag{14}$$

The parameter P_t, which parametrizes damped eigenmode strength, is determined from Eqs. (5) and (6) in terms of the expressions in Eqs. (7)–(14).

A. The threshold parameter P_t

Assuming $\gamma_2<0$, the threshold parameter P_t is given by[2]

$$P_t=\frac{D_1(C_2+C_3)}{C_1^2(2-\gamma_2/\gamma_1)}. \tag{15}$$

The parameter was derived to be an order of magnitude indicator that energy transfer involving a damped mode is roughly as large as the transfer between unstable modes whenever $P_t\approx 1$. Assuming that the second and third terms of the right hand side of Eq. (5) reach finite amplitude before the fourth term, it is formed from the ratio of those two terms to the first term, calculated when the linear instability γ_1 is saturated by the nonlinear term driven by C_1. The quantities in Eq. (15), which are functions of k and k', are assumed to lie in a range for which the wave number variation is not strong. Thus γ_1 and γ_2 are evaluated at the same k for simplicity and several combinations of k and k' (generally chosen near the maxima of the spectra) are checked to get a sense of typical variation of P_t with k. Experience with a reduced model for ITG turbulence has shown that when $P_t\gtrsim 0.4$, the damped and unstable eigenmodes have comparable fluctuation levels.[2]

Because the coupling coefficients C_1, C_2, and D_1 are formed from similar linear combinations of A_j and B_j, frequently $D_1(C_2+C_3)/C_1^2\approx 1$. When true, P_t is most sensitive to the growth rate ratio γ_2/γ_1. If $|\gamma_2|\gg|\gamma_1|$, $P_t\ll 1$ because the damped eigenmode is so heavily damped that its amplitude in saturation is very small. If $|\gamma_2|\sim|\gamma_1|$, the growth rates are optimal for strong excitation and γ_2 is a significant energy sink for saturation. From the properties of quadratic dispersion relations, a necessary and sufficient condition for modes with growth rates with opposite signs is $|b_r|<\rho^{1/2}|\cos(\phi/2)|$. When $|b_r|\ll\rho^{1/2}|\cos(\phi/2)|$, growth and damping rates are comparable. All models, except drift thermal turbulence and ionization driven turbulence, have $b_r>0$. With instability for $[-b_r+\rho^{1/2}|\cos(\phi/2)|]/2>0$, it is always possible for the system to be sufficiently close to threshold so that $|\gamma_2|=[b_r+\rho^{1/2}|\cos(\phi/2)|]/2\gg[-b_r+\rho^{1/2}|\cos(\phi/2)|]/2=\gamma_1$. This means that sufficiently near threshold, damped eigenmode effects are weak for two-field systems. For three-field systems, it is possible to have conjugate paired eigenmodes with a third neutral mode, such that growth and damping rates are matched near threshold.[17]

The structure of the models is such that damping effects associated with collisions typically govern Re Z_{11} and Re Z_{22} and, in some cases, Re Z_{12} and Re Z_{21}. If these are the only terms and collisional dissipation is positive in the sense that Re Z_{11} and Re Z_{22} are positive, there is no instability. Instability must then be driven by gradients of equilibrium quantities, which most often appear in Im Z_{12}, Im Z_{21}, and Im Z_{22}. Model variations also put gradient terms in Im Z_{11} and Re Z_{21}, but infrequently. When the system is unstable, the second root is usually damped. If the gradients are not sufficiently strong, the system lies slightly above threshold and

the damped eigenmode is strongly damped. Stronger gradients give growth and damping rates that are comparable. Strong gradients are associated with large diamagnetic frequencies. To summarize, robust gradient-driven instability in two-field systems is generally accompanied by a damped eigenmode with a comparable damping rate and the situation is reflected in large values for Im Z_{12}, Im Z_{21}, and Im Z_{22}.

Two models have regimes in which instability is driven by atomic processes represented by collisional coefficients with a negative sign.[15,16] These instabilities do not feed off the equilibrium gradients of common drift waves. Depending on the parameters, the damping rate of the damped eigenmode can be comparable to or larger than the growth rate. The strength of nonlinear coupling then determines whether the damped eigenmode plays a role in saturation.

We discuss situations in which the coefficients C_j and D_1 produce strong variations in P_t. In the combination $D_1(C_2+C_3)/C_1^2$, the factors C_1, C_2, C_3, and D_1 have almost identical expressions except for variation in the eigenvectors R_1 and R_2. This combination can be different from unity only when R_1 or R_2 assumes values that are greatly different from unity, in combination with either A_j or B_j vanishing. Furthermore, this combination is averaged over k', smoothing the wave number dependencies of R_1 and R_2, leaving the parametric dependencies to govern when these quantities are large or small. For the sake of discussion, assume that the coefficients A_j and B_j, if not zero identically, are all the same order of magnitude. There are four cases, two each for A-type and B-type nonlinearities. For A-type nonlinearities, $D_1(C_2+C_3)/C_1^2$ goes like $(A_1R_2-A_2R_2)(A_1R_1-A_2R_1)/(A_1R_1-A_2R_2)^2$. This is akin to a reduced mass $R_1R_2/(R_1-R_2)^2$, which yields $D_1(C_2+C_3)/C_1^2 \ll 1$ whenever R_1/R_2 is much greater than or much less than unity. For B-type nonlinearities, $D_1(C_2+C_3)/C_1^2$ reduces to something like $(B_1-B_2R_1^2)/(B_1-B_2R_1R_2)$, which too can be much larger or much smaller than unity for exceptional values of R_j. The four cases are summarized as follows: Case (1) $B_j=0$, $R_2 \gg R_1$; case (2) $B_j=0$, $R_1 \gg R_2$; case (3) $A_j=0$, $R_1 \gg 1$, $R_1 \gg R_2$; and case (4) $A_j=0$, $R_1R_2 \gg 1$, $R_2 \gg R_1$. In Sec. III we will note when parametric dependencies allow any of these situations to arise and the resulting effect on damped eigenmodes.

To verify the predictions of P_t, we look at the energy in saturation. The energy can be defined as proportional to $\Sigma_k|F_1(k)|^2+K(k)|F_2(k)|^2$, where K is a real function of wave number and model parameters. Eigenmode decomposition gives energy proportional to $\Sigma_k\{(|R_1|^2+K)|\beta_1|^2+(|R_2|^2+K)|\beta_2|^2+[2\,\mathrm{Re}(R_1^*R_2\langle\beta_1^*\beta_2\rangle+2K\,\mathrm{Re}\langle\beta_1^*\beta_2\rangle]\}$. The first term is the energy in the unstable modes, the second term is the energy in damped modes, and the last term is a mixed term containing both damped and growing mode amplitudes. The mixed term arises from nonorthogonal eigenmodes and can be large and either positive or negative. In analyzing the models, we compare the saturation energies of damped and growing modes and the energy injection and damping rates from the growing and stable modes to evaluate the relative importance of damped modes.

III. SATURATION CHARACTERIZATION

A. Trapped electron mode turbulence

TEM turbulence is a core fluctuation in tokamaks requiring that the collisional detrapping rate be less than the bounce frequency. The two-field reduction of TEM turbulence[8] has $F_1=\epsilon^{-1/2}n_{tr}+\phi_k$, where n_{tr} is the density of trapped electrons, F_2 is the electrostatic potential ϕ_k, and ϵ is the aspect ratio. The nonlinearities are electrostatic with $A_1=\mathbf{k}'\times\hat{\mathbf{z}}\cdot\mathbf{k}$ arising from E×B advection of the density and $A_2=\mathbf{k}'\times\hat{\mathbf{z}}\cdot\mathbf{k}[(k-k')^2-k'^2]/2(1+k^2-\epsilon^{1/2})$ arising from advection of the vorticity (k is normalized to the ion sound gyroradius ρ_s). The linear coupling coefficients are $Z_{11}=\nu$, $Z_{12}=-\nu+ik_yv_D\hat{\alpha}$, $Z_{21}=-\epsilon^{1/2}\nu/(1+k^2-\epsilon^{1/2})$, and $Z_{22}=[\epsilon^{1/2}\nu+ik_yv_D(1-\epsilon^{1/2}\hat{\alpha})]/(1+k^2-\epsilon^{1/2})$, where ν is the detrapping rate, v_D is the diamagnetic frequency, and $\hat{\alpha}$ is a parameter of order unity proportional to the electron density gradient drive. The eigenfrequencies are given by

$$\omega=\frac{k_yv_D(1-\hat{\alpha}\epsilon^{1/2})-i\nu(1+k^2)}{2(1+k^2-\epsilon^{1/2})}\pm\left\{\frac{[k_yv_D(1-\hat{\alpha}\epsilon^{1/2})-i\nu(1+k^2)]^2}{4[1+k^2-\epsilon^{1/2}]^2}+\frac{ik_yv_D\nu}{(1+k^2-\epsilon^{1/2})}\right\}^{1/2}. \tag{16}$$

The growth rates are comparable and of opposite sign if $\rho^{1/2}|\cos(\phi/2)| \gg b_r$, which translates to $k_yv_D \gg \nu$. This defines the weakly collisional regime, sometimes referred to as "collisionless." In this limit, Im $Z_{12} \approx$ Im $Z_{22} \gg$ Re Z_{11}, Re Z_{12}, Re Z_{21}, and Re Z_{22}. On the other hand, if $\nu \gg k_yv_D$ (dissipative regime), the damped mode has a damping rate proportional to ν, while the growth rate of the unstable mode is much smaller (proportional to $k_y^2v_D^2/\nu$). In this case, no imaginary part of Z_{ij} is larger than a real part. As a result, $(2-\gamma_2/\gamma_1)^{-1}$ is of order unity in the weakly collisional case and much smaller than unity in the dissipative case.

It remains to determine the ratio of coupling coefficients $D_1(C_2+C_3)/C_1^2$ in the two limits. In the weakly collisional limit, the eigenvector components go as $R_1 \sim \mathrm{O}(1)$, $R_2 \sim \mathrm{O}(k_yv_D/\nu) \gg 1$. With $R_2 \gg R_1$, the ratio of nonlinear coupling coefficients in P_t can assume values that are greater than unity. For turbulence whose spectrum is contained within a long wavelength range, $A_2 \ll A_1$. Furthermore, weak dispersion ($k^2 \ll 1$) leads to a situation in which $D_1/C_1 \sim \mathrm{O}(1)$ and $(C_2+C_3)/C_1 \sim \mathrm{O}(k_y^2v_D^2/\nu^2)$. P_t is larger than unity and the damped eigenmode is expected to saturate the linear instability. For a spectrum contained within a short

wavelength range where $A_2 \approx A_1$, $A_2 R_2$ dominates C_1, C_2, and C_3, while the lowest order term of R_1 governs D_1. The result is $(C_2+C_3)/C_1 \sim \mathrm{O}(1)$ and $D_1/C_1 \sim \mathrm{O}(\nu/k_y v_D)$. Now $P_t < 1$ and damped eigenmodes play a weaker role in saturation.

In the dissipative limit, the eigenvector coefficients are $R_1 \sim \mathrm{O}(1)$ and $R_2 \sim \mathrm{O}(1)$, leading to $(C_2+C_3)/C_1 \sim \nu/k_y v_D \gg 1$ and $D_1/C_1 \sim 1$ in the long wavelength limit. The nonlinear transfer to the damped eigenmode is strong, but the damping rate is so large that $(2-\gamma_2/\gamma_1)^{-1} \sim k_y^2 v_D^2/\nu^2$, making P_t small in spite of the strong coupling. The damped eigenmode is therefore expected to have a small amplitude in saturation relative to the growing eigenmode. In the short wavelength range, the nonlinear coupling is weaker.

Numerical evaluation of P_t in the weakly collisional limit and in an intermediate wave number range gives values of P_t that are slightly below unity. Specifically, $P_t = 0.39$ and 0.38 for $(k_x, k_y) = (0.5, 0.6)$ and $(0.2, -0.5)$, respectively. Here we have averaged P_t over k' as for all other models in this paper. For longer wavelengths, P_t is larger. Energy evolution in the weakly collisional regime for intermediate wave numbers has been shown in Fig. 2 of Ref. 8 and the figure confirms that the damped eigenmode reaches a level in saturation that is similar to that of the growing mode. In contrast, numerical evaluation of P_t in the dissipative limit yields values of 0.0058 and 0.048 for $(k_x, k_y) = (0.4, 0.6)$ and (0.2,0.5), respectively. In this case, the damped eigenmode energy is five orders of magnitude lower than the energy of the growing eigenmode.

More germane to the question of saturation is the rate of energy dissipation by the damped eigenmode compared to energy injection rate by the instability. These two rates are estimated as $\Sigma_k \gamma_1(k)(|R_1|^2+K)|\beta_1|^2$ and $|\Sigma_k \gamma_2(k)(|R_2|^2 + K)|\beta_2|^2|$, respectively, where $K = 1 + k^2 - \epsilon^{1/2}$. We show a direct comparison between these two rates in Fig. 1(a), which plots the ratio of these two energy rates versus ν/v_D. It is seen that these two rates are comparable over the weakly collisional regime. As collisions begin to dominate, the rate of energy dissipated by the damped eigenmode becomes smaller relative to the energy injection rate. The same data are plotted as a function of $-\gamma_2/\gamma_1$ in Fig. 1(b). Here we find the striking result that the energy rates remain in balance even as $-\gamma_2/\gamma_1$ increases to values of more than 100. This indicates that even when the damped eigenmode amplitude drops off as $|\gamma_2|$ increases well above γ_1, the drop off is offset by the increasing damping rate, keeping the dissipation rate in balance with energy injection rate. The damped mode not only achieves a significant level in the weakly collisional case, but it provides the primary energy sink for saturation.

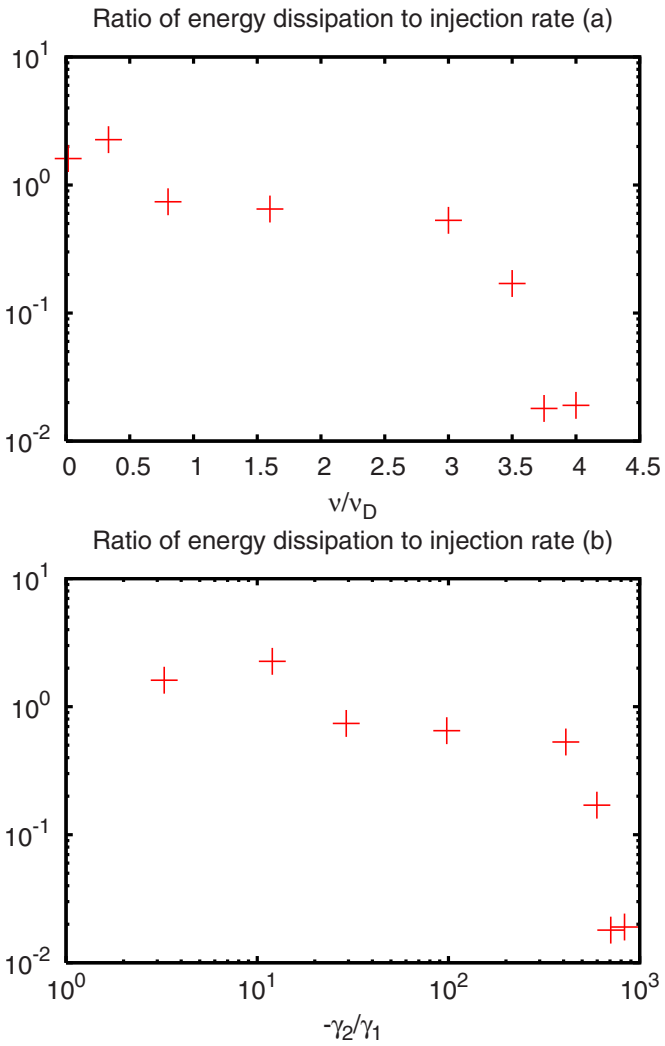

FIG. 1. (Color online) The ratio of energy dissipation rate by damped branch to energy injection rate by unstable branch. In (a), this ratio decreases as the collisional frequency increases in comparison to the diamagnetic frequency. In (b), it is seen that this effect is represented by the factor $-\gamma_2/\gamma_1$, which directly affects P_t.

B. Local Hasegawa–Wakatani turbulence

The Hasegawa–Wakatani (HW) model applies when the detrapping collision rate exceeds the bounce frequency. The larger collisionality relative to TEM makes this model relevant toward the edge of hot tokamaks or in colder plasmas.[18] This model has been widely studied,[19,20] but damped eigenmodes have not been considered. The fluctuation fields are the passing electron density for F_1 and electrostatic potential for F_2. Like the TEM model, the nonlinearities are electrostatic density advection in the density equation and advection of vorticity in the vorticity equation. The linear coupling coefficients are $Z_{11} = k_z^2 V_e^2/\nu_e + Dk^2$, $Z_{12} = -k_z^2 V_e^2/\nu_e + ik_y v_D$, $Z_{21} = -k_z^2 V_e^2/\nu_e k^2$, and $Z_{22} = k_z^2 V_e^2/\nu_e k^2 + \nu_{in} + \mu_{ii} k^2$, where V_e is the electron thermal velocity, ν_e is the electron collision rate, D is a collisional diffusivity of electron density, ν_{in} is an ion neutral drag, and μ_{ii} is an ion-ion viscosity.

Writing $k_z^2 V_e^2/\nu_e = \Omega_\parallel$, the eigenfrequencies are

$$\omega = -\frac{i}{2}\left[\Omega_\parallel\left(1+\frac{1}{k^2}\right) + Dk^2 + \nu_{in} + \mu_{ii}k^2\right] \pm \frac{i}{2}\left\{\left[\Omega_\parallel\left(1-\frac{1}{k^2}\right) + Dk^2 - \nu_{in} - \mu_{ii}k^2\right]^2 + (4\Omega_\parallel/k^2)(\Omega_\parallel - ik_y v_D)\right\}^{1/2}. \quad (17)$$

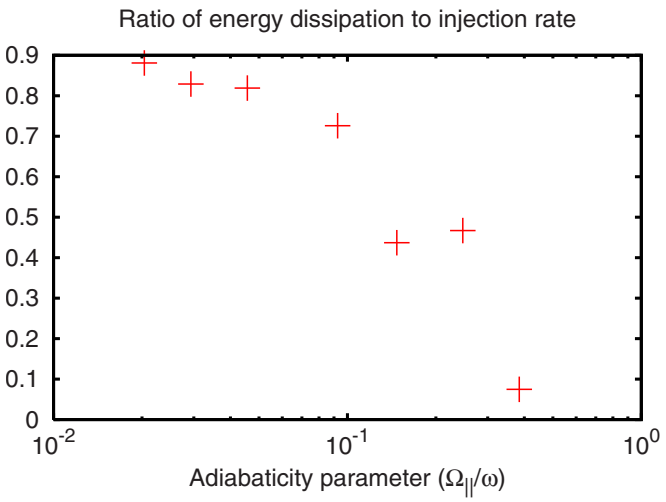

FIG. 2. (Color online) Ratio of damped branch energy dissipation rate to the unstable branch energy input rate as a function of the adiabaticity parameter for the Hasegawa–Wakatani model.

This dispersion leads to a nearly conjugate pair of eigenmodes if $k_y v_D \gg \Omega_{\|}$, Dk^2, ν_{in}, and μ_{ii},

$$\omega_{1,2} = \pm i\frac{(1-i)}{\sqrt{2}}\left(\frac{k_y v_D \Omega_{\|}}{k^2}\right)^{1/2} + \mathrm{O}(\Omega_{\|}). \tag{18}$$

The condition $\Omega_{\|} \ll k_y v_D$ can be rewritten using Eq. (18) to replace $k_y v_D$ by $\omega^2 k^2/\Omega_{\|}$, yielding $k_z^2 V_e^2/\nu_e \omega \ll k \approx 1$. The factor on the left of the inequality is known as the adiabaticity parameter and the inequality defines the hydrodynamic regime of HW. We find that the hydrodynamic regime has growing and damped eigenmodes with $-\gamma_2 \sim \gamma_1$. The conjugate pairing makes R_1 and R_2 comparable, leading to comparable coupling coefficients C_j and D_1. The parameter P_t is therefore expected to be order unity and the damped eigenmode is predicted to reach a significant level. Numerical evaluation of P_t yields values of 7.9 and 0.2 for $(k_x,k_y) = (0.3,1.1)$ and $(-0.1,0.2)$, respectively. In this regime, Im $Z_{12} \gg$ Re Z_{11}, Re Z_{12}, Re Z_{21}, and Re Z_{22}.

The limit $k_y \nu_D \lesssim \Omega_{\|}$ is known as the adiabatic limit. Here, Im Z_{12} is smaller than Re Z_{11}, Re Z_{12}, Re Z_{21}, or Re Z_{22}. When $|Dk^2 - \nu_{in} - \mu_{ii}k^2|$ is either much larger or much smaller than $|1-1/k^2|\Omega_{\|}$, both eigenmodes are damped. Otherwise there is an unstable mode whose growth rate is much smaller than the damping rate. Numerical evaluation of P_t yields values of 0.04 and 0.03 for $(k_x,k_y)=(0.1,-0.6)$ and $(-0.3,0.5)$, respectively.

Numerical simulation shows that the damped mode energy is comparable to the growing mode energy in the hydrodynamic regime and much smaller in the adiabatic regime, consistent with the calculated values of P_t in the two regimes. Dissipation rates behave in a like fashion as seen in Fig. 2. The damped eigenmode decay rate is nearly as large as the growing mode growth rate in the hydrodynamic regime and becomes much smaller as $k_z^2 V_e^2/\nu_e \omega$ becomes large.

In the local approximation $\nabla_{\|} \to ik_z$=constant, the HW and TEM models are very similar. Both models have terms in both equations proportional to the difference of density and potential. The constant of proportionality is the adiabaticity parameter (multiplied by ω) in HW and $\nu/k_y v_D$ in TEM. In both systems, when the constant of proportionality is large, n and ϕ must be nearly equal to maintain a balance with any other term in the equations. With $n \approx \phi$, the dynamics is reducible to a single field and dominated by a single eigenmode. When the parameter is small, n and ϕ are independent and two eigenmodes are present at finite amplitude. Both constants of proportionality directly relate to the linear coupling rule and P_t. It is well known that adiabaticity and hydrodynamic regimes are different. It is seen here that a crucial aspect of this difference is damped eigenmode dissipation, which saturates the turbulence in the hydrodynamic regime.

C. Drift thermal turbulence

This system models fluctuations in the tokamak scrape-off layer driven by atomic physics.[15] The fields F_1 and F_2 are the temperature and electrostatic potential. The nonlinearities are advection of temperature and vorticity, making them electrostatic A-type nonlinearities. The linear coupling coefficients are $Z_{11} = -\gamma_T + (2/3)\alpha^2 \chi k_z^2 + \chi_{\perp} k^2 + \chi_{\|} k_z^2$, $Z_{12} = -(2/3)\alpha\chi k_z^2 + ik_y v_{*T}$, $Z_{21} = -\chi\alpha k_z^2/k^2$, and $Z_{22} = \chi k_z^2/k^2$, where χ is the electron parallel resistive diffusivity, $\chi_{\perp}$ and $\chi_{\|}$ are perpendicular and parallel thermal conductivities, $\alpha = 1.71$ is a constant, γ_T represents the effect of radiative cooling, and v_{*T} is a diamagnetic velocity associated with temperature advection.[15] Radiative cooling makes a negative contribution to Re Z_{11}, allowing instability from negative dissipation. This model can also have instability through the diamagnetic frequency $k_y v_{*T}$, which appears in Im Z_{12}. If $k_y v_{*T}$ is large, Im Z_{12} is larger than the other components of Z_{ij}.

Simplifying notation with $\gamma_c \equiv \gamma_T - (2/3)\alpha^2 \chi k_z^2 - \chi_{\perp} k^2 - \chi_{\|} k_z^2$, the eigenfrequencies are

$$\omega_{1,2} = \frac{i}{2}\left(\gamma_c - \frac{\chi k_z^2}{k^2}\right) \pm \frac{i}{2}\left\{\left(\gamma_c + \frac{\chi k_z^2}{k^2}\right)^2 - 4\frac{\chi k_z^2 \alpha}{k^2}\left(ik_y v_{*T} - \frac{2}{3}\alpha\chi k_z^2\right)\right\}^{1/2}. \tag{19}$$

When $(4\chi k_z^2\alpha/k^2)(ik_y v_{*T} - 2\alpha\chi k_z^2/3)$ inside the radical is smaller than the other term $(\gamma_c + \chi k_z^2/k^2)^2$, the growth rate is $\gamma_1 \approx \gamma_c$ and the damping rate is $\gamma_2 \approx -\chi k_z^2/k^2$. This is the regime of the radiative cooling drive associated with negative Re Z_{11}. While the eigenvectors have $|R_1| \gg |R_2|$, this does not affect the factor $D_1(C_2+C_3)/C_1^2$, which stays close to unity. If $\gamma_c \gg \chi k_z^2/k^2$, the growth is stronger than damping and $P_t \sim 1$ is expected. Numerical evaluation gives $P_t = 0.72$ and 0.70 for $(k_x,k_y)=(0.6,0.4)$ and $(-0.2,0.9)$, respectively, indicating that damped modes are significant. If $\gamma_c \ll \chi k_z^2/k^2$, the damping becomes very strong and we should get $P_t \ll 1$. Numerically, P_t is 0.001 and 0.002 for $(k_x,k_y)=(0.5,-0.1)$ and (0.0,0.5).

Large diamagnetic frequency makes $(4\chi k_z^2\alpha/k^2)(ik_y v_{*T} - 2\alpha\chi k_z^2/3) \gg (\gamma_c + \chi k_z^2/k^2)^2$, resulting in almost equal growth and damping rates $\gamma_{1,2} \approx \pm(\chi k_z^2 \alpha k_y v_{*T}/2k^2)^{1/2}$, assuming $k_y v_{*T} \gg \alpha\chi k_z^2$. With matched growth and damping rates, $|R_1|$

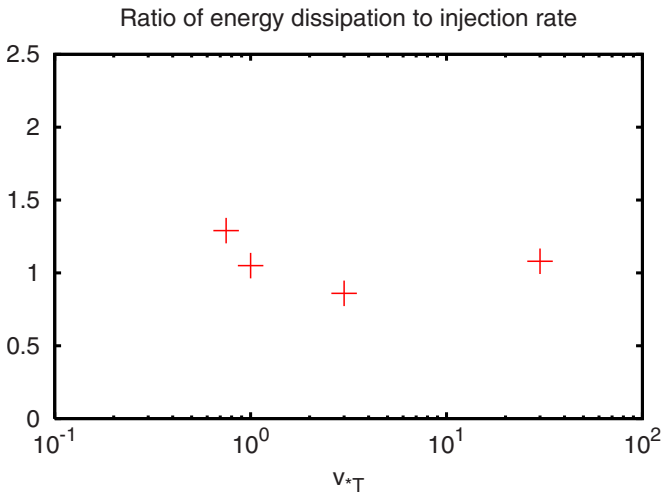

FIG. 3. (Color online) The damped branch energy dissipation rate compared to the unstable branch energy input rate as a function of the diamagnetic velocity for the drift thermal turbulence.

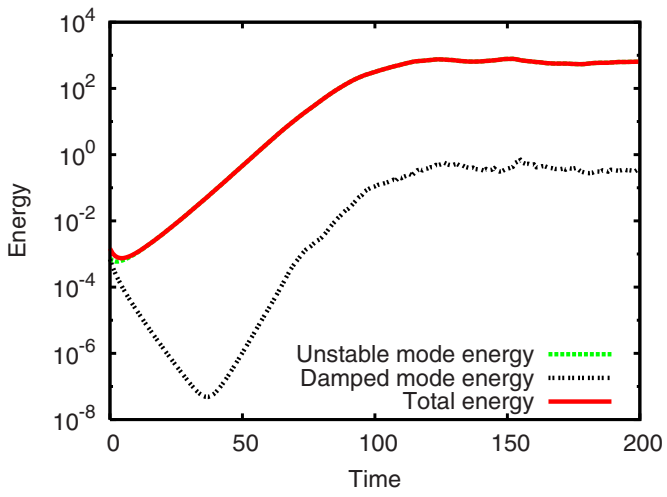

FIG. 4. (Color online) Evolution of energies for ionization driven drift wave turbulence in a regime driven by ionization. Although the damped eigenmode is excited, it saturates at a level that is nearly three orders of magnitude below the unstable mode.

$\sim|R_2|$, leading to $P_t=1.6$ and 0.51 for $(k_x,k_y)=(0.6,0.3)$ and $(-0.1,-0.4)$, respectively. Energy dissipation and injection rates are compared in Fig. 3. Their ratio is of order unity for a large range of diamagnetic velocities, which shows that damped modes saturate turbulence over a wide parameter range. For several points on this plot, the damping rate of the damped mode, which is proportional to $|\beta_2|^2$, is larger than the energy input rate of the instability (proportional to $|\beta_1|^2$). The difference arises because the nonorthogonality of the eigenmodes produces additional energy change through terms that are proportional to $\beta_1\beta_2^*$ and its complex conjugate. This change in the present case slightly enhances the energy injection rate, requiring the larger damping rate. The eigenmode cross-correlation terms are shown explicitly in Eqs. (31) and (33) of Sec. IV.

D. Ionization driven turbulence

Similar to the previous model, ionization driven turbulence describes fluctuations driven by atomic physics in the scrape-off layer of tokamaks.[16] The two fields of this model are parallel velocity for F_1 and electrostatic potential for F_2. The nonlinearities are advection of parallel flow and a nonlinearity in the F_2 equation that combines advection of electron density and vorticity.[21] These are A-type nonlinearities. The linear coupling coefficients are $Z_{11}=\gamma_{cx}+\mu k_z^2$, $Z_{12}=i(k_y v_{*v}+k_z c_s)$, $Z_{21}=ik_z c_s/(1+k^2\rho_s^2)$, and $Z_{22}=-(\gamma_I-Dk_y^2)/(1+k^2\rho_s^2)+ik_y v_{*\phi}/(1+k^2\rho_s^2)$, where γ_I and γ_{cx} are the ionization and charge exchange rates, μ is a parallel viscosity, $D=1.71v_\phi^2\eta_e/\chi_\parallel\bar{k}_z^2$, η_e is the ratio of electron density to temperature scale lengths, χ is the parallel thermal conductivity, k_z is an average parallel wave number, c_s is the ion sound speed, ρ_s is the ion sound gyroradius, $v_{*\phi}$ is the diamagnetic drift velocity, and v_{*v} is the diamagnetic drift velocity for parallel velocity. This model is like the drift thermal model and is different from the other models because instability can be driven by its negative values of dissipation. Here it is Re Z_{22} that can be negative, representing the destabilizing effect of ionization. However, the model can also have instability associated with large diamagnetic terms.

Defining $\gamma_c\equiv-\gamma_{cx}-\mu k_z^2-(Dk_y^2/\hat{b})+(\gamma_I/\hat{b})$ and $\hat{b}\equiv 1+k^2\rho_s^2$, the eigenfrequencies are

$$\omega_{1,2}=\frac{i}{2}\left(\gamma_c-\frac{ik_y v_{*\phi}}{\hat{b}}\right)\pm\frac{i}{2}\left\{\left(\gamma_{cx}+\mu k_z^2+\frac{\gamma_I-Dk_y^2-ik_y v_{*\phi}}{\hat{b}}\right)^2-4\frac{k_z c_s}{\hat{b}}(k_y v_{*v}+k_z c_s)\right\}^{1/2}. \quad (20)$$

The regime of ionization drive occurs when the term $[\gamma_{cx}+\mu k_z^2+(\gamma_I-Dk_y^2-ik_y v_{*\phi})/\hat{b}]^2$ is much larger than the other term inside the radical. This yields a growth rate $\gamma_1\approx(\gamma_I-Dk_y^2)/\hat{b}$ and a damping rate $\gamma_2\approx-\gamma_{cx}-\mu k_z^2$. If $Dk_y^2\lesssim\gamma_I$ and $\gamma_I\sim\gamma_{cx}$, the damping is very strong and $P_t(k,k')$ is around 10^{-5} for all (k,k') except $k_y'=0$. This implies that the damped modes do not play a strong role in saturation and this has been verified in simulations. If $\gamma_I\sim\gamma_{cx}\gg Dk_y^2,\mu k_z^2$, then the damping and growth rates are comparable. However, in this case $|R_2|\gg|R_1|$ and for A-type nonlinearities, this leads to $D_1(C_2+C_3)/C_1^2\ll 1$. As a result, P_t turns out to be similar to the case before and damped modes again do not play a role. This case is illustrated in Fig. 4 where the energy in damped modes is three orders of magnitude lower than the total energy. There is one more case when $\gamma_I\gg\gamma_{cx},Dk_y^2,\mu k_z^2$. Here, the growth is very strong compared to the damping but still $|R_2|\gg|R_1|$ leading to P_t values of around 10^{-5}. Thus stable modes do not affect saturation, as verified in simulations. Comparing to drift thermal turbulence, the other negative dissipation model, we note that both have regimes where the growing and damped modes have comparable rates. However, nonlinear coupling is sufficient to excite damped eigen-

modes to a significant level for drift thermal turbulence but not for ionization driven turbulence.

There is a regime of gradient-driven instability occurring when the term $[\gamma_{cx}+\mu k_z^2+(\gamma_I - Dk_y^2 - ik_y v_{*\phi})/\hat{b}]^2$ is much smaller than the other term inside the radical. Unlike the previous models, Re $Z_{12}=0$ and $Z_{12}Z_{21}$ is real and negative provided both k_y and k_z are positive. This causes both modes to be damped or growing depending on the sign of γ_c. A second diamagnetic regime occurs when $k_y v_{*v}$ is the largest rate. If k_z is negative relative to k_y, there is a pair of growing and damped eigenmodes with comparable rates. The nonlinear coefficient ratio $D_1(C_2+C_3)/C_1^2$ is also of order unity, giving P_t values of order unity. Numerical evaluation gives $P_t=0.72$ and 0.43 for $(k_x,k_y)=(0.4,-0.4)$ and $(-0.1,0.2)$, respectively. Numerical solutions confirm that the damped and growing eigenmode energies are comparable in saturation.

This model is complicated for its negative dissipation and two diamagnetic frequencies. In the appropriate strong gradient regime, it does have significant damped eigenmode activity, like the other models. In the regime of negative dissipation, instability damped eigenmode activity hinges on nonlinear coupling strengths.

E. Local resistive interchange turbulence

The local resistive interchange instability is driven by pressure gradients and is relevant at the edge of tokamaks and stellarators. It is a three-field electromagnetic model[11] involving the poloidal flux, electrostatic potential, and pressure, but it can be reduced to a two-field electrostatic model by neglecting the induced electric field. The electrostatic case, which we study here, has F_1 as the pressure, F_2 as the electrostatic potential, and A-type nonlinearities arising from advection of pressure and vorticity. The linear coupling coefficients are $Z_{11}=0$, $Z_{12}=ik_y dP_0/dr$, $Z_{21}=-i\kappa k_y/k^2$, and $Z_{22}=k_z^2/\eta k^2$, where P_0 is the equilibrium pressure, κ is the curvature, and η is the resistivity. With $Z_{11}=0$ and Z_{22} real, this mode does not have negative dissipation. Like ionization driven turbulence it does have Re $Z_{12}=$Re $Z_{21}=0$, but the product $Z_{12}Z_{21}$ is positive and real. Consequently instability is driven by the pressure gradient which, when weak, gives weak instability with a heavily, unimportant damped eigenmode, and when strong gives a regime in which the damped mode is important. The latter corresponds to $(\mathrm{Im}\, Z_{12})\times(\mathrm{Im}\, Z_{21})>(\mathrm{Re}\, Z_{22})^2$.

The dispersion relation is $\omega^2+i(k_z^2/\eta k^2)\omega+\kappa(k_y^2/k^2)\times(dP_0/dr)=0$ and the roots are

$$\omega_{1,2}=\frac{-i}{2}\left(\frac{k_z^2}{\eta k^2}\right)\pm\frac{i}{2}\left\{\left(\frac{k_z^2}{\eta k^2}\right)^2+4\frac{dP_0}{dr}\frac{\kappa k_y^2}{k^2}\right\}^{1/2}. \tag{21}$$

Instability requires that $\kappa(dP_0/dr)>0$, where dP_0/dr is taken as a constant parameter. When $\kappa(k_y^2/k^2)(dP_0/dr)\ll k_z^4/\eta^2 k^4$ then $-\gamma_2\gg\gamma_1$. In this case $R_1\gg R_2$ and with A-type nonlinearities, this leads to $D_1(C_2+C_3)/C_1^2\sim 1$. Because of this, numerical evaluation of P_t gives values of 0.0003 and 0.001 for the wave numbers $(k_x,k_y)=(-0.4,-0.7)$ and $(0.1,-0.8)$, respectively. In the situation when $k_z^4/\eta^2 k^4\ll\kappa(k_y^2/k^2)(dP_0/dr)$, the eigenfrequencies are given by

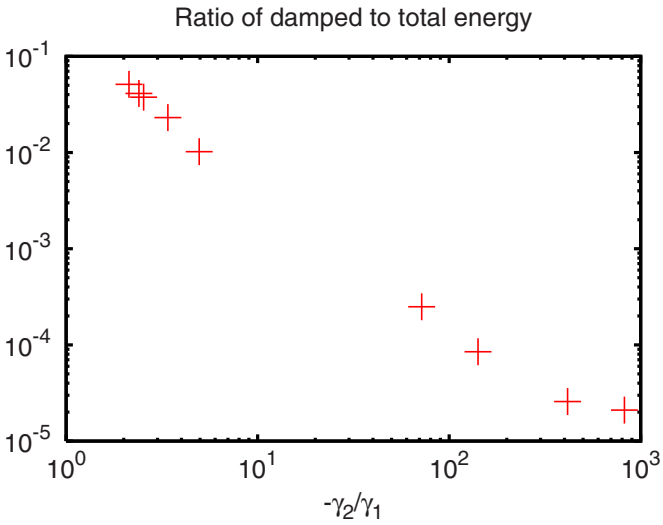

FIG. 5. (Color online) For resistive interchange turbulence, the damped mode amplitude decays as the ratio $-\gamma_2/\gamma_1$ for the most linearly unstable mode is increased.

$$\omega_{1,2}\simeq\frac{-i}{2}\left(\frac{k_z^2}{\eta k^2}\right)\pm\frac{i}{2}\left(\frac{dP_o}{dr}\frac{4k_y^2\kappa}{k^2}\right)^{1/2}\pm\frac{i}{4}\frac{k_z^4/\eta^2 k^4}{[(dP_0/dr)(4k_y^2\kappa/k^2)]^{1/2}}. \tag{22}$$

In this case, $-\gamma_2\sim\gamma_1$ and $|R_1|\sim|R_2|$. This gives P_t values of 2.7 and 0.6 for the wave numbers $(k_x,k_y)=(0.4,0.3)$ and $(-0.3,0.1)$, respectively. Thus damped modes are expected to play a role in saturation of turbulence. Both these cases have been verified in simulations. Figure 5 shows this by plotting the ratio of energy in damped modes to total energy, while in saturation, as the ratio $-\gamma_2/\gamma_1$ is increased by decreasing the driving gradient dP_0/dr. As predicted by P_t, damped mode amplitude decreases as the driving gradient is lowered, with the damped mode unimportant for large values of $-\gamma_2/\gamma_1$.

F. Rayleigh–Taylor turbulence

The Rayleigh–Taylor instability is driven by pressure gradients in regions of bad field-line curvature.[22] A two-field model for turbulence driven by this instability was studied in Ref. 10, where saturation was described in conventional terms by a cascade to small scales, aided by the shearing of zonal flows. We show here that the damped eigenmode is strongly excited and provides an energy sink in the wave number range of the instability. The model has equations for plasma density represented by F_1 and potential represented by F_2, with A-type nonlinearities describing advection of density and vorticity. The linear coupling coefficients are $Z_{11}=Dk^2+ik_y v_g$, $Z_{12}=ik_y(v_n-v_g)$, $Z_{21}=-ik_y v_g/k^2$, and $Z_{22}=\mu k^2$, where D is a collisional diffusion coefficient of density, μ is the viscosity, v_g is a normalized gravitational drift arising through curvature, and v_n is the diamagnetic drift. Like the resistive interchange model, this model has positive dissipation Re $Z_{12}=$Re $Z_{21}=0$ and $Z_{12}Z_{21}$ real and positive

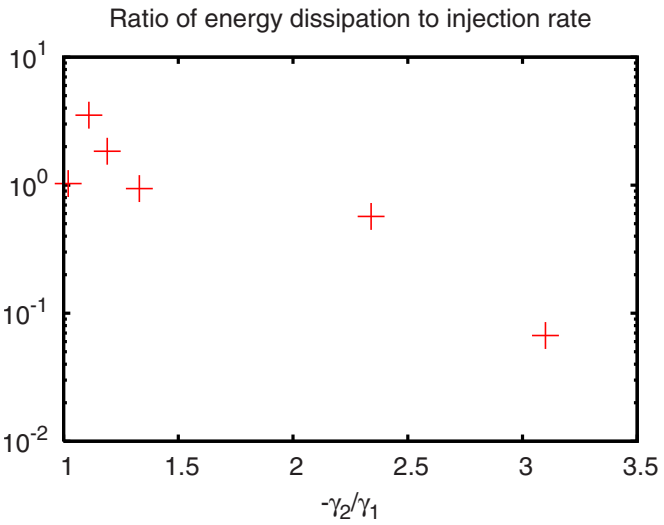

FIG. 6. (Color online) Ratio of damped branch energy dissipation rate to unstable branch energy input rate for the Rayleigh–Taylor model as the ratio $-\gamma_2/\gamma_1$ is increased. This ratio is increased by decreasing the driving term $v_n - v_g$.

(when $v_n > v_g$). Consequently, turbulence is driven by the gravity and gradient drift terms residing in the imaginary parts of Z_{ij}.

The dispersion relation is $\omega^2 + i(Dk^2 + \mu k^2 + ik_y v_g)\omega - \mu k^2(Dk^2 + ik_y v_g) + (k_y^2/k^2)v_g(v_n - v_g) = 0$, with roots given by

$$\omega = \frac{k_y v_g - i(\mu + D)k^2}{2} \pm \frac{i}{2}\left\{[(D-\mu)k^2 + ik_y v_g]^2 + \frac{4v_g k_y^2}{k^2}[v_n - v_g]\right\}^{1/2}. \tag{23}$$

When $[(D-\mu)k^2]^2$ is larger than $k_y^2 v_g^2$ or $4(k_y^2/k^2)v_g(v_n - v_g)$, both eigenmodes are damped with damping rates $\gamma_1 = -\mu k^2$ and $\gamma_2 = -Dk^2$. When $[(D-\mu)k^2]^2 \ll |4(k_y^2/k^2)v_g(v_n - v_g) - k_y^2 v_g^2|$, there is a pair of unstable and stable eigenmodes that form a conjugate pair in lowest order, with second order dissipative terms breaking the conjugate symmetry. The eigenfrequencies are

$$\omega_{1,2} \approx \frac{k_y v_g}{2} \mp \frac{v_g(D-\mu)k^2}{2[4v_g(v_n - v_g)/k^2 - v_g^2]^{1/2}} \pm i\frac{k_y}{k}\{v_g[(v_n - v_g) - v_g k^2/4]\}^{1/2} - \frac{i}{2}(D+\mu)k^2. \tag{24}$$

With $-\gamma_2 \approx \gamma_1$, R_1 and R_2 are comparable, as are the coupling coefficients D_1 and C_j. We therefore expect that P_t is nearly unity and that the damped eigenmode plays a significant role in saturation. This is confirmed from numerical evaluation of P_t, which gives values of 0.55 and 0.27 for wave numbers of $(k_x, k_y) = (0.6, -0.2)$ and $(-0.1, -0.4)$, respectively. Figure 6 shows that the damped modes sink most of the energy input by the instability when the ratio $-\gamma_2/\gamma_1$ is between 1 and 1.5. As in Fig. 3, nonorthogonal eigenmodes increase the dissipation rate beyond that produced by $|\beta_1|^2$, making the damping rate larger than the unstable eigenmode injection rate for some of the data points. However, unlike Fig. 1(b) where the energy rates remain in balance for a large range of $-\gamma_2/\gamma_1$, in this case the energy dissipation by damped modes becomes insignificant as $-\gamma_2/\gamma_1$ goes over 3.

G. Two-field ion temperature gradient turbulence

ITG turbulence is driven by an electrostatic instability associated with the ion pressure gradient.[12] It plays a major role in ion confinement in tokamaks. Damped eigenmodes in ITG have been examined for a three-field model and gyrokinetics. Because there is a two-field ITG model, we briefly examine it in connection with the other types of turbulence studied here. This model is useful for tracking zonal flows. The relationship between zonal flows and saturation by damped eigenmodes will be described elsewhere.

This model has ion pressure for F_1 and electrostatic potential for F_2. The nonlinearities are type A, corresponding to advection of pressure and vorticity. The linear coupling coefficients are $Z_{11} = \chi k^4$, $Z_{12} = ik_y(1+\eta_i)$, $Z_{21} = -i\epsilon k_y/(1+k^2)$, and $Z_{22} = (\nu k^2 + ik_y)/(1+k^2)$, where χ is a coefficient of collisional hyperdiffusion of pressure, $\eta_i = d(lnT_i)/d(lnn)$ is the ratio of density gradient scale length to ion temperature gradient scale length, ϵ is the ratio of density gradient scale length to magnetic field variation scale length, and ν is the dissipation of flow active at large scales. With Re Z_{11} and Re Z_{22} positive, the system is unstable through η and can be expected to have a damped mode damping rate that is comparable to the growth rate when the instability is above threshold.

The dispersion relation is $\omega^2(1+k^2) + \omega[i\chi k^4(1+k^2) - k_y + i\nu k^2] - i\chi k_y k^4 - \nu\chi k^6 + \epsilon k_y^2(1+\eta_i) = 0$ and the roots are

$$\omega_{1,2} = -\frac{i}{2}\left(\chi k^4 + \frac{\nu k^2 + ik_y}{1+k^2}\right) \pm \frac{i}{2}\left\{\left(\chi k^4 - \frac{\nu k^2 + ik_y}{1+k^2}\right)^2 + \frac{4(1+\eta_i)k_y^2\epsilon}{1+k^2}\right\}^{1/2}. \tag{25}$$

If $[\chi k^4 - (\nu k^2 + ik_y)/(1+k^2)]^2 \gg (1+\eta_i)k_y^2\epsilon/(1+k^2)$, then both roots are damped with damping $\gamma_1 \approx -\nu k^2/(1+k^2)$ and $\gamma_2 \approx -\chi k^4$. If η_i is larger than the other parameters, then we get approximately equal growth and damping rates $\gamma_{1,2} \approx \pm[(1+\eta_i)k_y^2\epsilon/(1+k^2)]^{1/2}$. In this case, the eigenvectors R_1 and R_2 have nearly equal magnitude and so P_t is expected to be close to unity. Numerical calculation of P_t gives 0.35 and 0.66 for the wave numbers $(k_x, k_y) = (0.1, 0.3)$ and $(-0.5, -0.5)$, respectively. Figure 7 shows the verification of this prediction where the energy in damped modes is very close to the total energy.

H. Microtearing turbulence with time-dependent thermal force

This model was introduced to provide a minimal two-field description of magnetic turbulence in magnetically confined plasmas. Although the fluctuations have been labeled microtearing, they are two-dimensional and require the TDTF for instability.[13] Without the TDTF, the fluctuations are stable and correspond to collisionally damped, counter-

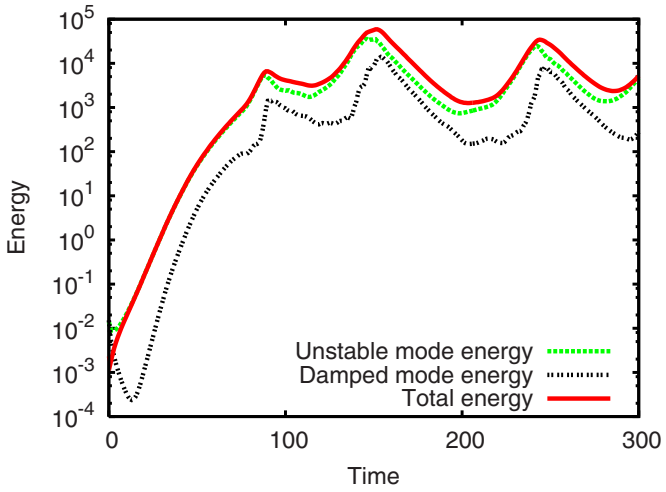

FIG. 7. (Color online) Evolution of energies for the two-field ITG model in a parameter regime where η is large.

propagating kinetic Alfvén waves.[23] The model has electron density for F_1 and the parallel component of the magnetic vector potential for F_2. The nonlinearites are magnetic and of type B. They correspond to the gradient of electron pressure along the perturbed magnetic field in Ohm's law (F_2 equation) and compression of electron flow along the perturbed field in the density continuity equation (F_1 equation). The linear coupling coefficients are $Z_{11}=\mu k^2$, $Z_{12}=-ik_z k^2$, $Z_{21}=-ik_z/[1-i(\alpha\alpha'/\nu_e)k_y dT_0/dx]$, and $Z_{22}=[\eta k^2-ik_y(1+\alpha)dT_0/dx]/[1-i(\alpha\alpha'/\nu_e)k_y dT_0/dx]$, where μ is a collisional density diffusivity, α and α' are the order unity coefficients of the thermal and time-dependent thermal forces, ν_e is the electron collision frequency, T_0 is the electron temperature, and η is the resistivity. This model has positive dissipation. Instability from the TDTF introduces imaginary components of $Z_{12}Z_{21}$ and Z_{22} and should therefore lead to growing and damped modes with comparable rates when the instability is above threshold.

The dispersion relation is given by $\omega^2(1-ik_y\alpha_T)+i\omega[(\mu+\eta)k^2-ik_y(\hat{\alpha}+\alpha_T\mu k^2)]-k_z^2k^2-\mu k^2(\eta k^2-ik_y\hat{\alpha})=0$. Here $\hat{\alpha}\equiv(1+\alpha)(dT_0/dx)$ and $\alpha_T\equiv(\alpha\alpha'/\nu_e)(dT_0/dx)$. The roots of this equation are

$$\omega_{1,2}=-\frac{i}{2}\left[\mu k^2+\frac{k_y^2\hat{\alpha}\alpha_T+\eta k^2+i(\eta k^2k_y\alpha_T-k_y\hat{\alpha})}{1+k_y^2\alpha_T^2}\right]\pm\frac{i}{2}\left\{\left[\mu k^2-\frac{k_y^2\hat{\alpha}\alpha_T+\eta k^2+i(\eta k^2k_y\alpha_T-k_y\hat{\alpha})}{1+k_y^2\alpha_T^2}\right]^2-4k_z^2k^2\left(\frac{1+ik_y\alpha_T}{1+k_y^2\alpha_T^2}\right)\right\}^{1/2}. \quad (26)$$

When $k_z^2k^2, k_y^2\alpha_T^2 \gg \mu k^2, \eta k^2, k_y\hat{\alpha}$, then the eigenfrequencies become

$$\omega_{1,2}\approx\mp\frac{k_zk}{(1+k_y^2\alpha_T^2)^{1/2}}\left[\frac{1+(1+k_y^2\alpha_T^2)^{1/2}}{2}\right]^{1/2}\mp\frac{ik_zk}{(1+k_y^2\alpha_T^2)^{1/2}}\left[\frac{-1+(1+k_y^2\alpha_T^2)^{1/2}}{2}\right]^{1/2}. \quad (27)$$

In this case, Im Z_{12} is larger than the real part of all Z's and so the growth and damping rates are almost equal. The eigenvectors R_1 and R_2 have comparable magnitudes which should lead to P_t values of close to unity. Numerical evaluation of P_t gives 1.1 and 0.23 for wave numbers $(k_x,k_y)=(0.6,0.2)$ and $(-0.4,-1.0)$, respectively. We therefore expect damped modes to play a prominent part in saturation for this case. If $k_y^2\alpha_T^2 \lesssim \mu k^2, \eta k^2, k_y\hat{\alpha}$, there is no instability drive as both modes are damped.

I. Thermal microtearing turbulence

Thermal microtearing turbulence is a variant of microtearing turbulence driven by the TDTF that couples magnetic fluctuations to temperature fluctuations.[14] This model becomes quite complicated when put in the standard form of Eqs. (1) and (2). The electron temperature fluctuation T is F_1, while F_2 is a linear combination of temperature and parallel component of magnetic vector potential ψ given by $F_2=[1-i(\alpha\alpha'/\nu_e)k_y dT_0/dx]\psi-i(\alpha\alpha'/\nu_e)k_zT$. The nonlinearities of the F_1 equation are A, B, and G-type; for F_2 they are B and G-type. The linear coefficients are

$$Z_{11}=(2/3)(\kappa/n_0)k_z^2+(2/3)(\alpha\alpha'/\nu_e)k_z^2\times[T_\alpha+iT'_\kappa]/[1-i(\alpha\alpha'/\nu_e)k_y dT_0/dx],$$

$$Z_{12}=(2/3)k_z[T'_\kappa-iT_\alpha],$$

$$Z_{21}=-ik_z(1+\alpha)+i(\alpha\alpha'/\nu_e)k_z\times[\eta k^2-ik_y(T_0/n_0)dn_0/dx-ik_y\times(1+\alpha)dT_0/dx]/[1-i(\alpha\alpha'/\nu_e)k_y dT_0/dx],$$

and

$$Z_{22}=[\eta k^2-ik_y(T_0/n_0)dn_0/dx-ik_y\times(1+\alpha)dT_0/dx]/[1-i(\alpha\alpha'/\nu_e)k_y dT_0/dx],$$

where $T_\alpha=(1+\alpha)(T_0/n_0)k^2$, $T'_\kappa=(\kappa/n_0)k_y dT_0/dx$, κ is the collisional parallel thermal conductivity, n_0 is the equilibrium density, and the remaining quantities are the same as those of microtearing turbulence (Sec. III H).

The TDTF drive appears in every linear coefficient except Z_{12}, making it difficult to infer eigenmode properties solely from inspection of Z_{ij}. The frequency expression is also sufficiently complicated that little is learned from inspection. Numerical evaluation shows that when k_z is an appreciable fraction of k_y and $(\alpha\alpha'/\nu_e)>(1+\alpha)$, there is a pair of growing and damped roots with $-\gamma_2<\gamma_1$. The eigenvector components have similar magnitude so that P_t is order unity. The damped eigenmode is therefore expected to play a significant role in saturation.

IV. SATURATION ENERGETICS

Damped eigenmodes saturate instabilities by damping the injected energy. We examine the nature of this damping. If energy conservation by the nonlinearities N_1 and N_2 takes the form

$$\int [\mathrm{Re}(F_1^* N_1) + K(k)\mathrm{Re}(F_2^* N_2)] d^2k = 0,$$

where $K(k)$ is a real function of wave number and parameters, the nonlinearly conserved energy is $E=(1/2)[|F_1|^2 + K(k)|F_2|^2]$. We now consider the part of the time rate of change of E that is governed by the linear coefficients Z_{ij}. Whereas the nonlinear terms are conservative, the linear terms are nonconservative and serve to inject energy into the fluctuation spectrum or to remove it. The time rate of change of energy by these nonconservative processes is given by

$$\left.\frac{dE}{dt}\right|_{nc} = -\mathrm{Re}[Z_{12}\langle F_2 F_1^*\rangle] - K(k)\mathrm{Re}[Z_{21}\langle F_1 F_2^*\rangle] - \mathrm{Re}\, Z_{11}|F_1|^2 - K(k)\mathrm{Re}\, Z_{22}|F_2|^2. \quad (28)$$

The first two terms on the right hand side are proportional to the correlation between the two fields. This correlation also governs the transport flux. The second two terms arise from collisional dissipation of F_1 and F_2. When Re Z_{11} and Re Z_{22} are positive, these terms damp fluctuation energy and instability comes from the cross-correlation. For the drift thermal and ionization drift wave models Re Z_{11} and Re Z_{22} could have negative values, in which case instability could be driven by the second two terms.

To separate the roles of unstable and stable eigenmodes, we express the right hand side in terms of the eigenmode amplitudes using the eigenmode decomposition $F_1 = R_1(k)\beta_1 + R_2(k)\beta_2$ and $F_2=\beta_1+\beta_2$, yielding

$$\left.\frac{dE}{dt}\right|_{nc} = \mathcal{C}_u + \mathcal{C}_s + \mathcal{D}_u + \mathcal{D}_s. \quad (29)$$

Here,

$$\mathcal{C}_u = -[\mathrm{Re}(Z_{12}R_1^*) + K(k)\mathrm{Re}(Z_{21}R_1)]|\beta_1|^2 \quad (30)$$

is the cross-correlation term associated with the unstable eigenmode,

$$\mathcal{C}_s = -[\mathrm{Re}(Z_{12}R_2^*) + K(k)\mathrm{Re}(Z_{21}R_2)]|\beta_2|^2 - \mathrm{Re}[Z_{12}(R_1^*\langle\beta_1^*\beta_2\rangle + R_2^*\langle\beta_1\beta_2^*\rangle)] - K(k)\mathrm{Re}[Z_{21}(R_1\langle\beta_1\beta_2^*\rangle + R_2\langle\beta_1^*\beta_2\rangle)] \quad (31)$$

is the cross-correlation term associated with stable eigenmode excitation,

$$\mathcal{D}_u = -[\mathrm{Re}(Z_{11})|R_1|^2 + K(k)\mathrm{Re}(Z_{22})]|\beta_1|^2 \quad (32)$$

is the collisional dissipation term associated with the unstable eigenmode, and

$$\mathcal{D}_s = -[\mathrm{Re}(Z_{11})|R_2|^2 + K(k)\mathrm{Re}(Z_{22})]|\beta_2|^2 - 2\,\mathrm{Re}\, Z_{11}\,\mathrm{Re}(R_1R_2^*\langle\beta_1\beta_2^*\rangle) - 2K(k)\mathrm{Re}\, Z_{22}\,\mathrm{Re}\langle\beta_1\beta_2^*\rangle \quad (33)$$

is the collisional dissipation term associated with stable eigenmode excitation.

The conventional view of saturation does not account for damped eigenmodes, effectively assuming that $\beta_2=0$ and making $\mathcal{C}_s=\mathcal{D}_s=0$. For conventional saturation $\Sigma_k\mathcal{C}_u=-\Sigma_k\mathcal{D}_u$, with $\mathcal{C}_u$ typically large and positive at large scales and $\mathcal{D}_u$ large and negative at small scales. Prior work based on selected fluid models[1,2,5] has shown that $\mathcal{C}_s$ is not zero, but negative and a significant fraction of $\mathcal{C}_u$. In this case, the transport flux is significantly reduced from the quasilinear value by the damped eigenmode contribution to the correlation that governs transport. When $\mathcal{C}_s$ is a significant fraction of $\mathcal{C}_u$, damped eigenmodes are said to play a role in saturation. This statement refers to saturation of the *linear instability*, which is represented by $\mathcal{C}_u$. In fact, $\mathcal{C}_s\neq 0$ can equally well be described as a finite-amplitude reduction of the instability growth rate from its linear value associated with $\mathcal{C}_u$. The difference $\mathcal{C}_u-|\mathcal{C}_s|$, which sets the reduced growth rate due to the damped eigenmode at finite amplitude, must still be saturated. This is accomplished by $\mathcal{D}_u+\mathcal{D}_s$. In gyrokinetic models for the cyclone base case[24] of ITG turbulence, there are a very large number of damped eigenmodes.[4] Some of these modes have values of $|\mathcal{C}_s|$ that are a significant fraction of $\mathcal{C}_u$. However, their effect is not systematic; there are positive and negative values in roughly equal measure, such that in a sum over the eigenmode spectrum, the net value of $\mathcal{C}_s$ is close to zero. In this situation, the probability distribution of $\mathcal{C}_s$ peaks near zero, i.e., it has a near zero mean value, even though it is broad.[3] The transport flux, which is proportional to the mean value of $\mathcal{C}_u+\mathcal{C}_s$ is therefore not very different from the quasilinear flux (which is proportional to $\mathcal{C}_u$). In the gyrokinetic models, $\mathcal{D}_s$ is both large and systematic in its effect, so that damped eigenmodes govern saturation primarily through collisional dissipation.

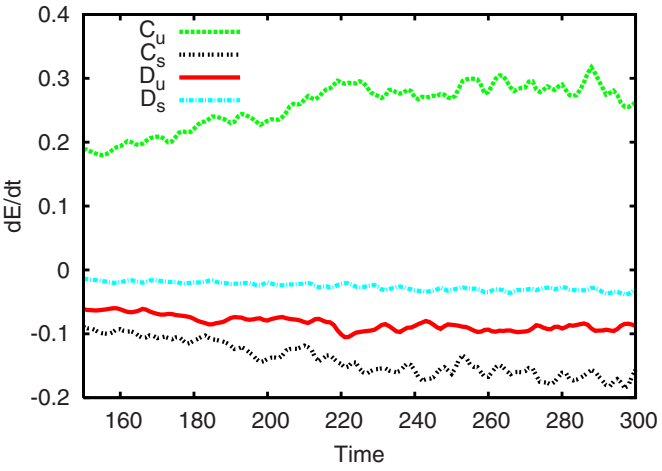

FIG. 8. (Color online) Cross-correlation and collisional contributions to energy dissipation broken into the components associated with the unstable and stable eigenmodes. This result is from the Rayleigh–Taylor model.

The situation for two-field fluid models is quite different, as depicted in Figs. 8 and 9, which give the values of $\mathcal{C}$ and $\mathcal{D}$ for Rayleigh–Taylor $[K(k)=1]$ and ion temperature gradient turbulence $[K(k)=1+k^2]$. In both cases, the most significant damped eigenmode effect resides in the cross-correlation. The damped eigenmode also contributes to the collisional dissipation at a level somewhat weaker than the contribution of the unstable eigenmode. These results are consistent with a large reduction of the quasilinear flux. This is illustrated in Fig. 10, which shows the quasilinear and true

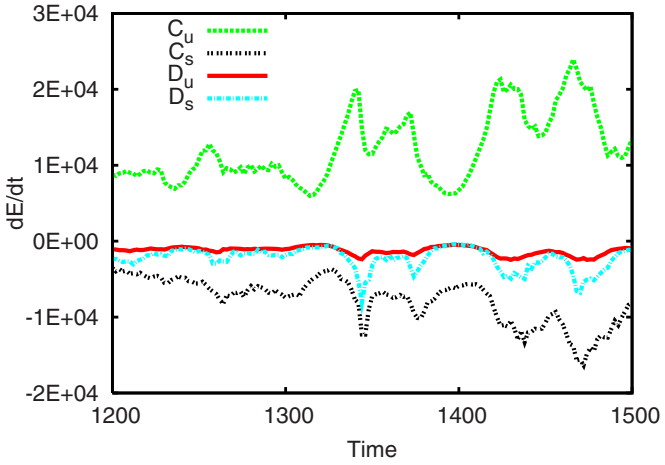

FIG. 9. (Color online) Cross-correlation and collisional contributions to energy dissipation broken into the components associated with the unstable and stable eigenmodes. This result is from the ITG model.

fluxes for both the hydrodynamic and adiabatic regimes of Hasegawa–Wakatani turbulence. In the former, there is a considerable reduction, consistent with strong excitation of the damped eigenmode. Three-field fluid models for ITG and ETG turbulence also have a significant systematic deviation of $\mathcal{C}_s$ from zero, and a correspondingly large reduction of the flux.

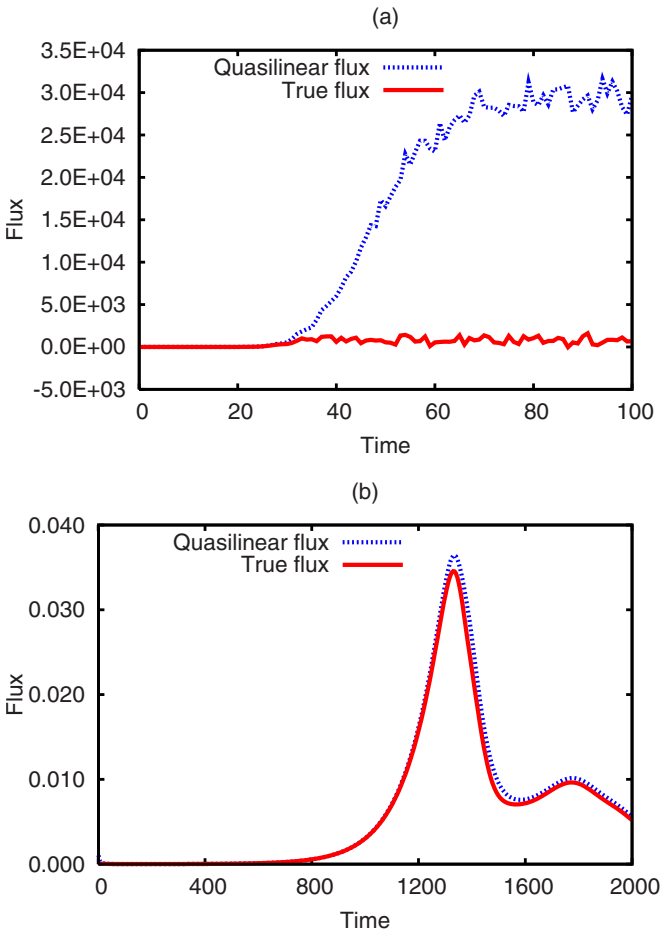

FIG. 10. (Color online) Comparison of fluxes in Hasagawa–Wakatani turbulence. In (a), the quasilinear flux is 35 times the true flux while in (b), the two fluxes are almost equal. Plot (a) is for the hydrodynamic regime in which damped modes are significantly excited, whereas (b) is for adiabatic regime in which damped modes are unimportant.

V. CONCLUSIONS

Nine two-field fluid models for instability-driven plasma turbulence covering different regimes of physics and parameters have been found to have commonplace regimes where damped eigenmodes saturate the linear instability. The damped eigenmodes are zeros of the dispersion relation. With the exception of TEM,[8] their role as the energy sink for saturation has not been described. It is concluded, therefore, that the involvement of damped eigenmodes in saturation is not unique to a certain type of instability process or parameter regime, but a natural adjunct to instability in turbulence driven by instability. For two-field fluid reductions, the quadratic dispersion makes damped eigenmodes more prominent when the instability is well above threshold and for strong diamagnetic frequency. When damped eigenmodes play a dominant role in saturation, the energy dissipation rate of the damped eigenmode is comparable to the energy injection rate. The saturation levels of stable and unstable eigenmodes are similar in many cases. Saturation by damped eigenmodes involves an energy sink in the energy-containing wave number range of the instability. Consequently, damped eigenmodes cannot be ignored in the descriptions of saturation, the steady state, or transport. This is important because damped eigenmodes are found to provide the energy sink for saturation in extensively studied systems where they were not previously identified, such as Rayleigh–Taylor, resistive interchange, and Hasegawa–Wakatani turbulence. We note that shear flows have been included as an entity apart from the instability in representations of some of these systems.[10] However, they have not been envisaged as, or play the role of, the primary energy sink. The interesting interaction between shear flows and damped eigenmodes will be described in future work.

A previously derived threshold parameter for saturation by damped eigenmodes P_t is found to be reliable for all nine models. When this parameter reaches values of a few tenths, damped eigenmodes become the dominant saturation mechanism. The parameter depends on the ratio of the damping rate to the growth rate and indicates that when the damped eigenmode damping rate is too large, energy flowing to small scales on the unstable wave number manifold will instead saturate the instability according to the conventional picture of saturation. The ratio of coupling coefficients between wave numbers on the unstable manifold and modes across the two manifolds also affects the value of P_t. This coupling ratio is often of order unity, but can be significantly different in certain cases described here.

It is found that the energy dissipation rate of the damped eigenmode remains similar to the energy injection rate when the ratio of damping to growth γ_2/γ_1 is not much greater than unity. If the magnitude of γ_2 is too large, the energy flowing to small scale on the unstable wave number manifold will saturate the instability and the unstable eigenmode dissipation will become small. For trapped electron mode tur-

bulence, the damped eigenmode dominates saturation even when γ_2/γ_1 is as large as 100. This reflects the large coupling coefficient between unstable and stable eigenmodes.

For all nine models, the damped eigenmode significantly changes the cross phase between the two fields from the value associated with the unstable eigenmode. This means that fluctuation energy is reabsorbed into the equilibrium gradients through the damped eigenmode in an inverse of the instability process. The transport flux is correspondingly reduced. This process can be viewed as a finite-amplitude-induced reduction of the energy injected into the spectrum by the instability; however, in this picture, the instability is no longer linear. The stable eigenmode also contributes to the damping arising from collisional dissipation terms. In the overall energetics this is a smaller effect than the change in energy evolution associated with the cross phase.

ACKNOWLEDGMENTS

The authors acknowledge contributions from Sangeeta Gupta, whose verification that damped eigenmode activity occurs in the Rayleigh–Taylor model hinted at a far more pervasive effect than then established. This work was supported by the U.S. Department of Energy through Grant No. DE-FG02-89ER53291.

[1]R. Gatto, P. W. Terry, and D. A. Baver, Phys. Plasmas **13**, 022306 (2006).
[2]P. W. Terry, D. A. Baver, and S. Gupta, Phys. Plasmas **13**, 022307 (2006).
[3]D. R. Hatch, P. W. Terry, W. M. Nevins, and W. Dorland, Phys. Plasmas **16**, 022311 (2009).
[4]D. R. Hatch, P. W. Terry, F. Jenko, F. Mertz, and W. M. Nevins, submitted.
[5]J.-H. Kim and P. W. Terry, Phys. Plasmas **17**, 112306 (2010).
[6]A. N. Kolmogorov, Dokl. Akad. Nauk SSSR **30**, 9 (1941).
[7]G. Falkovich and K. Sreenivasan, Phys. Today **59** (4), 43 (2006).
[8]D. A. Baver, P. W. Terry, R. Gatto, and E. Fernandez, Phys. Plasmas **9**, 3318 (2002).
[9]C. Holland, G. R. Tynan, J. H. Yu, A. James, D. Nishijima, M. Shimada, and N. Taheri, Plasma Phys. Controlled Fusion **49**, A109 (2007).
[10]A. Das, S. Mahajan, P. Kaw, A. Sen, S. Benkadda, and A. Verga, Phys. Plasmas **4**, 1018 (1997).
[11]B. A. Carreras, L. Garcia, and P. H. Diamond, Phys. Fluids **30**, 1388 (1987).
[12]C. Holland, P. H. Diamond, S. Champeaux, E. Kim, O. Gurcan, M. N. Rosenbluth, G. R. Tynan, N. Crocker, W. Nevins, and J. Candy, Nucl. Fusion **43**, 761 (2003).
[13]A. B. Hassam, Phys. Fluids **23**, 38 (1980).
[14]G. G. Craddock and P. W. Terry, Phys. Fluids B **3**, 3286 (1991).
[15]A. S. Ware, P. H. Diamond, B. A. Carreras, J.-N. Leboeuf, and D. K. Lee, Phys. Fluids B **4**, 102 (1992).
[16]A. S. Ware, P. H. Diamond, H. Biglari, B. A. Carreras, L. A. Charlton, J.-N. Leboeuf, and A. J. Wootton, Phys. Fluids B **4**, 877 (1992).
[17]P. W. Terry, D. A. Baver, and D. R. Hatch, Phys. Plasmas **16**, 122305 (2009).
[18]G. R. Tynan, C. Holland, J. H. Yu, A. James, D. Nishijima, M. Shimada, and N. Taheri, Plasma Phys. Controlled Fusion **48**, S51 (2006).
[19]A. Hasegawa and M. Wakatani, Phys. Rev. Lett. **50**, 682 (1983).
[20]F. Y. Gang, P. H. Diamond, J. A. Crotinger, and A. E. Koniges, Phys. Fluids B **3**, 955 (1991).
[21]P. W. Terry and W. Horton, Phys. Fluids **25**, 491 (1982).
[22]H. Takabe and A. Yamamoto, Phys. Rev. A **44**, 5142 (1991).
[23]P. W. Terry and K. W. Smith, Phys. Plasmas **15**, 056502 (2008).
[24]A. M. Dimits, G. Bateman, M. A. Beer, B. I. Cohen, W. Dorland, G. W. Hammett, C. Kim, J. E. Kinsey, M. Kotschenreuther, A. H. Kritz, L. L. Lao, J. Mandrekas, W. M. Nevins, S. E. Parker, A. J. Redd, D. E. Shumaker, R. Sydora, and J. Weiland, Phys. Plasmas **7**, 969 (2000).